Strange-metal behavior in $PrAu_2In_4$ with a pseudodoublet ground state

Zhaotong Zhuang,[1,2,*] Meng Lyu,[1,*] Te Zhang,[1,2] Xiaoci Zhang,[1,2] Hengcan Zhao,[1] Junsen Xiang,[1] Shuai Zhang,[1,2,3,†] and Peijie Sun[1,2,3,‡]

[1]*Beijing National Laboratory for Condensed Matter Physics, Institute of Physics, Chinese Academy of Sciences, Beijing 100190, China*

[2]*School of Physical Sciences, University of Chinese Academy of Sciences, Beijing 100049, China*

[3]*Songshan Lake Materials Laboratory, Dongguan, Guangdong 523808, China*

(Received 19 October 2023; revised 27 May 2024; accepted 23 July 2024; published 5 August 2024)

Single crystals of the quasi-one-dimensional $PrAu_2In_4$ have been successfully grown and studied down to very low temperatures. Consistent with the singlet spin-orbit ground state of Pr^{3+}, no magnetic ordering is observed in this compound. Nevertheless, $PrAu_2In_4$ reveals a strong magnetic instability arising from the nearly degenerate ground and low-lying singlets that are spaced by only 9 K (termed the pseudodoublet), laying a ground for the competition among crystal field energy, magnetic exchange interaction, and Kondo physics. Moderate Kondo effect comparable to the pseudodoublet spacing is evidenced by a comparative investigation of specific heat and thermopower between $PrAu_2In_4$ and $LaAu_2In_4$. Notably, at $T > 2$ K, $PrAu_2In_4$ can be smoothly tuned by field to a strange-metal state near 1 T that is reminiscent of quantum critical fluctuations. At the lowest temperatures of $T < 1$ K, however, such quantum fluctuations are quenched and the compound behaves consistently as a Fermi liquid. The strange-metal behavior visible solely at elevated temperatures is considered generic to Kondo lattices with pseudodoublet ground state of non-Kramers ions, characterized by closely spaced singlets.

DOI: 10.1103/PhysRevB.110.085108

I. INTRODUCTION

Heavy fermion and the related quantum states have been at the forefront of strongly correlated electron phenomena for decades [1,2]. The underlying physics roots in the hybridization of local spin and conduction band, which has been intensively studied for Ce- and Yb-based intermetallics with one f electron or hole per rare-earth ion, known as magnetic Kramers ion. Rare-earth or actinide ions with two f electrons, like $Pr^{3+}(4f^2)$ and $U^{4+}(5f^2)$, often exhibit atypical heavy-fermion physics due to the diversity of the spin-orbit ground-state multiplet. Prototypical examples include URu_2Si_2 with a hidden-order phase [3], $PrOs_4Sb_{12}$ [4], and PrT_2Zn_{20} (T = Ir, Rh) [5] that reveal superconductivity derived from quardupolar rather than spin fluctuations. Different to the Kramers ions of trivalent Ce^{3+} ($4f^1$) and Yb^{3+} ($4f^{13}$), Pr^{3+} or U^{4+} with an even number of f electrons is free of Kramers theorem. Their eigenstates are therefore not protected by time-reversal symmetry and the spin-orbit ground-state multiplet might be magnetic or nonmagnetic depending on the surrounding crystal electric field (CEF).

Thus far, Pr-based correlated intermetallics with high structural symmetry have been of primary research interest due to the incidental multipolar degeneracy and the resultant cooperative order. For example, $PrOs_4Sb_{12}$ and PrT_2Zn_{20} are cubic and have nonmagnetic doublet ground state characterized by quadrupolar instability. Their low-symmetry counterparts, which are more likely to have a singlet spin-orbit ground state, have been seemingly too naive to be of interest. This work focuses on such a system, $PrAu_2In_4$, which belongs to a quasi-one-dimensional (q1D) family of RAu_2In_4 (R = La, Ce, Pr, and Nd) crystallizing in $NdRh_2Sn_4$-type orthorhombic structure (space group *Pnma*, No. 62) [6–9]. The crystal structure features R-R chains running along the q1D axis, surrounded by alternatively stacked Au_2In_3 pentagons and Au_3In_5 octagons, see Fig. 1(a). Previous studies on this compound revealed no magnetic ordering, despite the Curie-Weiss (CW) type magnetic susceptibility observed at $T > 50$ K indicative of local magnetic moments of Pr^{3+} (Ref. [6]).

In $PrAu_2In_4$, the Hund's rule multiplet of Pr^{3+} ion ($L = 5$, $S = 1$, and $J = 4$) subject to orthorhombic CEF splits into nine nonmagnetic singlets [10]. Given a nonmagnetic singlet ground state, the lack of magnetic ordering can be readily understood. However, if the ground and the lowest-lying singlets are closely spaced, the interplay between the CEF and exchange fields can gives rise to distinct magnetic behaviors —an old topic in rare-earth intermetallics [11]. Consequently, nearly degenerate singlets with accidental dipolar or quadrupolar degrees of freedom may arise, as previously discussed for $PrCu_2$ [12]. Such pseudomultiplet systems are typically characterized by enhanced low-energy magnetic excitations albeit the absence of magnetic ordering.

Here, we report on the successful synthesis of single crystals of $PrAu_2In_4$ and its nonmagnetic analog $LaAu_2In_4$, followed by a comprehensive low-T investigation including magnetic susceptibility, resistivity, specific heat, thermal expansion, and thermopower. For $PrAu_2In_4$, a pseudodoublet ground state with an energy spacing of ∼9 K is evidenced, accompanied by a moderately enhanced electronic

*These authors contributed equally to this work.
†Contact author: szhang@iphy.ac.cn
‡Contact author: pjsun@iphy.ac.cn

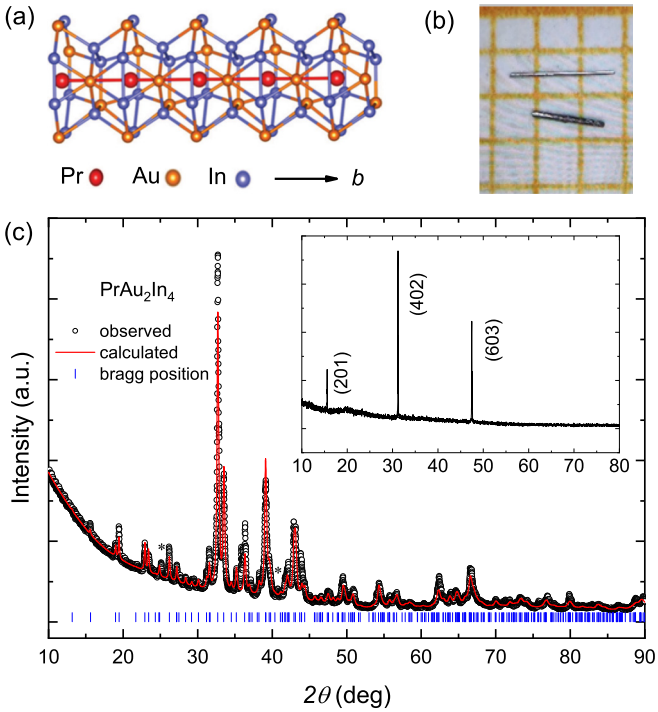

FIG. 1. (a) Polyhedral unit of $PrAu_2In_4$ lattice extending along b axis. (b) Optical image of the as-grown, needlelike single crystals of $PrAu_2In_4$. (c) Powder x-ray diffraction pattern of selected single-crystal needles, as compared to the calculated one. Asterisks mark unidentified reflections. Inset shows the x-ray diffraction measured on an as-grown facet corresponding to the (201) plane.

specific-heat coefficient $\gamma \sim 70$ (± 20) mJ mol^{-1} K^{-2}, considerably larger than $\gamma = 5$ mJ mol^{-1} K^{-2} observed in $LaAu_2In_4$. Likewise, the low-T thermopower S exhibits an initial slope S/T differing by a factor of about 20 between the two compounds. At finite temperatures of $T > 2$ K and near 1–2 T, a field-tuned strange-metal state with non-Fermi-liquidlike behavior manifests in $PrAu_2In_4$, though neither magnetic ordering nor a quantum critical point takes place. Upon cooling down to below about 1 K, however, this compound settles down to Fermi liquid for all applied fields, in line with the nonmagnetic nature of the singlet CEF ground state. These observations distinguish $PrAu_2In_4$ from typical heavy-fermion compounds, elucidating its unique temperature- and field-dependent correlated electron physics that is driven by the competition between the Kondo effect and exchange coupling in a pseudodoublet system of non-Kramers ion.

II. EXPERIMENTAL DETAILS

Single crystals of $PrAu_2In_4$ and $LaAu_2In_4$ were grown from molten indium as reported previously [6,8]. High-purity elements Pr/La, Au, and In, mixed in a molar ratio of 1 : 2 : 20, were loaded into an alumina crucible and sealed in an evacuated quartz tube. The sealed quartz tube was slowly heated up to 1000 °C in 10 h, dwelling for 72 h, and then cooled down to room temperature over 240 h. After removing the excess indium by centrifugation at 350 °C, needle-shaped single crystals of $PrAu_2In_4$ and $LaAu_2In_4$, 1–4 mm in length along b axis, were obtained [see Fig. 1(b)]. Prior to the physical properties measurements, the single crystals were immersed in hydrochloric acid (diluted with deionized water at a volume ratio 1:4) for 1 h to remove traces of remaining indium on the surface. X-ray diffraction measurement was performed on powdered samples as well as single-crystal facets to confirm the $NdRh_2Sn_4$-type crystal structure, as has been done for $CeAu_2In_4$ [8].

Dc magnetic susceptibility and magnetization measurements were performed using a magnetic property measurement system (MPMS, Quantum Design) between 2 and 300 K, and further down to 0.4 K by incorporating a ^{3}He insert (iHelium3). Electrical resistivity and specific-heat measurements were carried out down to 0.3 K in an Oxford ^{3}He refrigerator by the four-wire and the thermal-relaxation method, respectively. Thermal expansion and magnetostriction were measured down to 2 K and up to 9 T in a physical properties measurement system (PPMS, Quantum Design) by using a capacitance dilatometer. Thermopower was measured by using a homemade thermal stage consisting of one heater and two thermometers within the PPMS.

III. RESULTS AND DISCUSSION

Figure 1(c) shows the powder x-ray diffraction pattern of carefully selected single-crystal needles, in comparison with the calculated one based on the $NdRh_2Sn_4$-type structure. Due to the small size of the single crystals, a large number of crystals had to be selected and ground for powder x-ray measurement. This process may have introduced trace amounts of unknown phases, possibly leading to the presence of faint unidentified peaks marked with asterisks in Fig. 1(c). The lattice constants determined by matching the measured and calculated patterns are $a = 18.5286(8)$ Å, $b = 4.6378(3)$ Å, and $c = 7.4015(6)$ Å, respectively. Single crystallinity is further confirmed by x-ray diffraction from the as-grown single-crystal facet parallel to the needle [Fig. 1(c) inset], from which the crystal orientation can be determined.

Isothermal magnetization $M(B)$ measured at $T = 0.4$ K [Fig. 2(a)] clearly demonstrates a uniaxial magnetic anisotropy in $PrAu_2In_4$: M for $B \parallel b$ attains 2.90 μ_B/f.u. at 7 T, close to the saturation moment $\mu_s = g_J J = 3.2$ μ_B/f.u. (the Landé factor $g_J = 0.8$) of free Pr^{3+} ion. By contrast, for $B \perp b$, M is one order of magnitude smaller, indicative of Ising-like moments aligning along the q1D direction (b axis). Despite the large magnetic moment and strong magnetic anisotropy, no metamagneticlike anomaly can be detected in the $M(B)$ curves, hinting at a nonmagnetic ground state.

Figure 2(b) shows the dc susceptibility $\chi(T)$ measured in a field of $B = 0.1$ T for $PrAu_2In_4$. Upon cooling, $\chi(T)$ increases continuously and shows largely different values at low temperatures for fields $B \parallel b$ and $B \perp b$, with $\chi_{\parallel b}/\chi_{\perp b} \approx 18$ at 1.8 K. The inverse susceptibility $\chi^{-1}(T)$, shown in Fig. 2(b) inset, well follows the modified CW law $\chi = \chi_0 + C_0/(T - \theta_P)$ at $T > 200$ K. Here, χ_0 is a temperature-independent susceptibility, C_0 the Curie constant and θ_P the paramagnetic Weiss temperature. The effective moment μ_{eff} estimated from C_0 is 3.69 μ_B and 3.59 μ_B for $B \parallel b$ and $B \perp b$, respectively, both close to the theoretical value $\mu_{\text{eff}} = g_J\sqrt{J(J+1)} = 3.58$ μ_B of free Pr^{3+} ion. The very different Weiss temperatures of 63.7 K ($B \parallel b$) and -28.3 K ($B \perp b$) manifest the

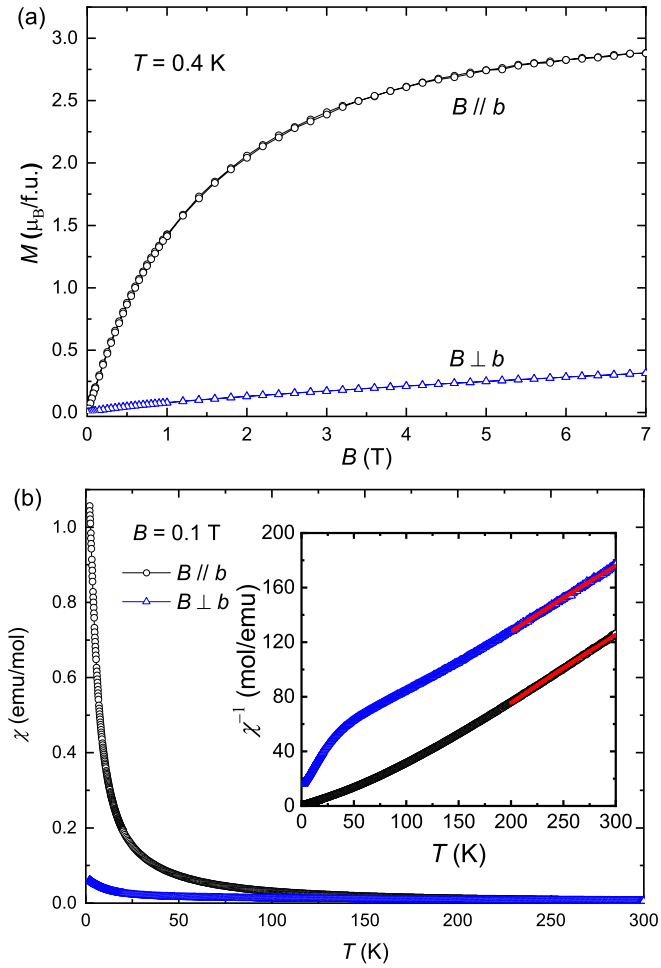

FIG. 2. (a) Isothermal magnetization $M(B)$ of $PrAu_2In_4$ measured for $B \parallel b$ and $B \perp b$ at $T = 0.4$ K. (b) Magnetic susceptibility $\chi(T)$ measured under 0.1 T for both field orientations. Inset: $\chi^{-1}(T)$ with the CW fitting (red lines), see text.

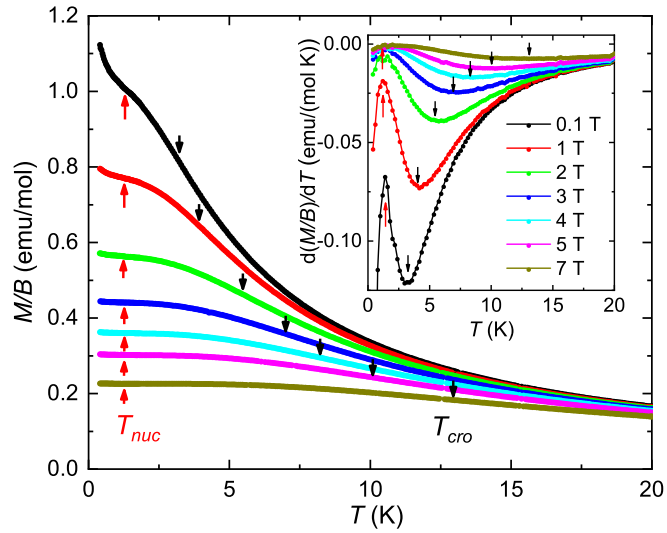

FIG. 3. Low-temperature $M(T)/B$ measured in varied magnetic fields oriented along b. The downward arrow locates the crossover at T_{cro} from high-T CW-like to low-T VV susceptibility, and the upward arrow marks $T_{\rm nuc}$ below which nuclear susceptibility appears on top of the flat VV contribution. Inset shows the corresponding values of $\mathrm{d}(M/B)/\mathrm{d}T$ vs T, where the aforementioned characteristic temperatures are determined by minima and maxima, respectively.

strong magnetocrystalline anisotropy of Pr^{3+} determined by the CEF, as detected by the anisotropic $M(B)$ [Fig. 2(a)].

As shown in Fig. 3, upon cooling the CW-like susceptibility evolves into a shoulder at low temperatures, with the crossover located by $\mathrm{d}(M/B)/\mathrm{d}T$ minimum at T_{cro}, as marked by downward arrow in Fig. 3 inset. Considering the all-singlet CEF scheme of the spin-orbit multiplet of Pr^{3+}, the weakly T-dependent, large $M(T)/B$ below T_{cro} can be ascribed to the Van Vleck (VV) paramagnetic contribution originating from the closely-spaced ground and low-lying singlets subject to strong interlevel coupling. Similar behavior has been observed in other Pr-based compounds such as $PrNi_2Al_5$ (Ref. [10]) with orthorhombic site symmetry resembling $PrAu_2In_4$, and even in cubic $PrMgNi_4$, where the degeneracy of the ground-state doublet is lifted by atomic disorder [13]. Moreover, T_{cro} shifts to higher temperature almost linearly with field as expected for Zeeman splitting, signaling the magnetic nature of the pseudodoublet state.

At low fields and below T_{cro}, an upturn superposed onto the flat VV behavior is observed, constituting an S-shaped behavior in $M(T)/B$. This upturn is better identified by the $\mathrm{d}(M/B)/\mathrm{d}T$ maximum at $T_{\rm nuc}$ (marked by upward arrow in Fig. 3 inset). Is the S-shape, or specifically, the low-temperature, upturn a hallmark of magnetic ordering of $4f$ electrons? It is apparently unlikely: $T_{\rm nuc} \approx 1.4$ K is highly robust to field up to at least 7 T, despite a gradually weakening intensity of the upturn feature. Furthermore, the energy gap between the ground and lowest-lying singlet is estimated to be $\Delta_E = 9$ K by analyzing the specific heat (see below), much higher than $T_{\rm nuc}$, rendering a magnetic order unrealistic. Instead, we interpret this $M(T)/B$ upturn as the CW susceptibility of Pr nuclear spin, akin to the observation made in $PrMg_3$ below about 1 K (Refs. [14,15]). Indeed, an enhanced nuclear susceptibility in Pr-based nonmagnetic intermetallics has long been known and interpreted in terms of the large hyperfine field generated by $4f$ electrons with significant VV susceptibility [16].

Normalized resistivity $\rho(T)/\rho_{300\mathrm{K}}$ in a wide temperature range of 0.3–300 K is shown in Fig. 4(a) for $PrAu_2In_4$ and $LaAu_2In_4$. The rather low resistivity ratio $\rho_{300\mathrm{K}}/\rho_{0.3\mathrm{K}}$ (8.7 and 5.0) in both compounds might arise from the potential atomic disorder in these compounds, given that Pr/La, Au, and In have the same Wyckoff symmetry (4c) [6,8]. Distinction between the two compounds is seen only at temperatures below about 150 K. As revealed by $\Delta\rho$ vs T ($\Delta\rho = \rho - \rho_0$, with ρ_0 being the residual resistivity), an inflection appears below 5 K in the resistivity of $PrAu_2In_4$, in rough accord with T_{cro} observed in $M(T)/B$. Fitting the resistivity at $T < 1.2$ K, i.e., well below the inflection, to the Fermi liquid (FL) description $\Delta\rho = A\,T^2$ yields $A = 1.2 \times 10^{-2}$ $\mu\Omega\,\mathrm{cm\,K^{-2}}$. Despite the singlet ground state, the A coefficient of $PrAu_2In_4$ appears to be greatly enhanced compared to the nonmagnetic counterpart, $LaAu_2In_4$. In the latter compound, the FL description applies below about 10 K, with a nearly two-order-of-magnitude smaller A coefficient, 2.26×10^{-4} $\mu\Omega\,\mathrm{cm\,K^{-2}}$.

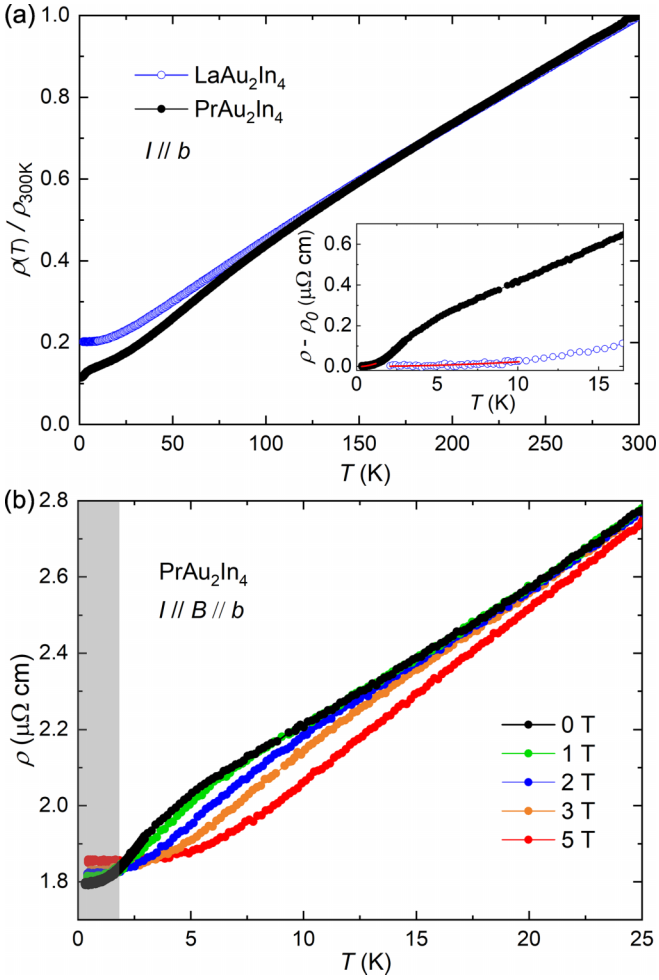

FIG. 4. (a) Normalized resistivity $\rho(T)/\rho_{300\mathrm{K}}$ measured in zero field for $PrAu_2In_4$ and $LaAu_2In_4$, with current applied along b axis (the needle direction). Inset shows the low-T closeup of $\Delta\rho = \rho - \rho_0$ and the FL fitting (red lines). (b) Low-T $\rho(T)$ of $PrAu_2In_4$ measured in varied fields. The shaded regime marks the temperature window where the ground-state singlet dominates.

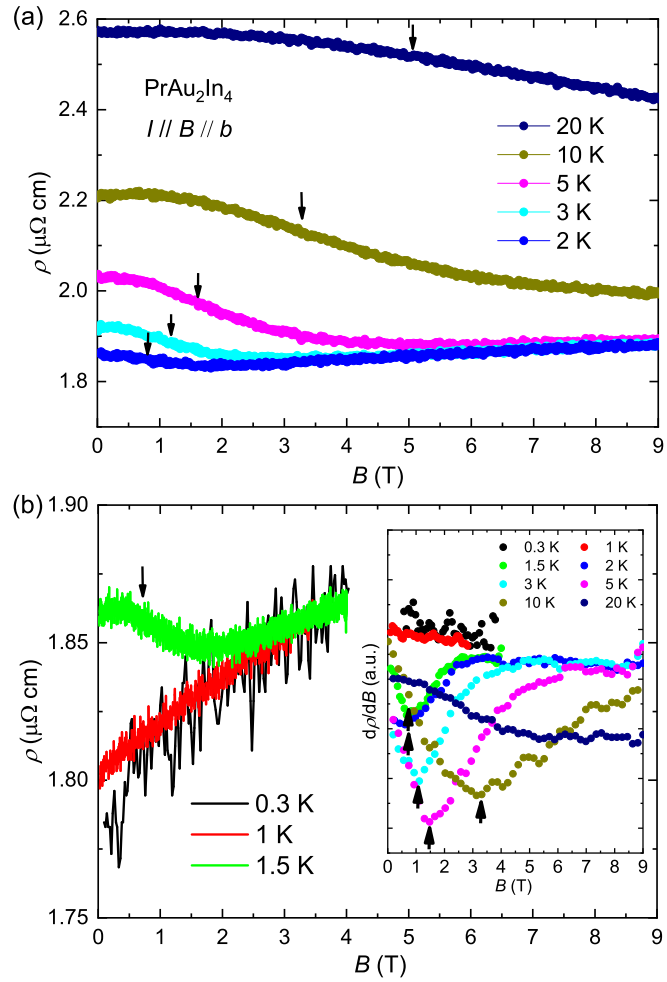

FIG. 5. Isothermal resistivity $\rho(B)$ of $PrAu_2In_4$ measured at varied temperatures [(a): $T \geqslant 2$ K; (b): $T \leqslant 1.5$ K] with both current and field applied along b axis. Inset shows $\mathrm{d}\rho/\mathrm{d}B$, where arrows mark the minima at B^* that correspond to the inflections in $\rho(B)$ curves.

Remarkably, the low-T $\rho(T)$ recorded in varying fields offers strong experimental evidence for the existence of strange-metal behavior at finite temperatures: Focusing on the temperature window 2–10 K, the $\rho(T)$ profile changes smoothly from negative curvature for $B = 0$ T to positive one for $B = 3$ T, see Fig. 4(b). Here, the curvature is quantified by the second derivative $\mathrm{d}^2\rho/\mathrm{d}T^2$ and will be shown below. Consequently, an approximately T-linear resistivity with zero curvature indicative of strange metal is expected for the intermediate fields between 1 and 2 T, whereas T-quadratic dependence characterizing heavy-fermion behavior is restored for higher fields. Such a field-induced crossover is, however, not seen at $T < 2$ K, where a T-quadratic resistivity persists irrespective of the applied field [see the shaded regime in Fig. 4(b)].

Supporting the field-tuned strange-metal behavior at elevated temperatures, the isothermal resistivity $\rho(B)$, shown in Figs. 5(a) and 5(b), exhibits a change reminiscent of a field-induced quantum critical regime, as observed in antiferromagnetic $YbRh_2Si_2$ (Ref. [17]). Specifically, $\rho(B)$ drops markedly at a characteristic field B^* that is identified by the $\mathrm{d}\rho/\mathrm{d}B$ minimum [Fig. 5(b) inset], with B^* shifting to higher field upon warming. As a probable explanation, the $\rho(B)$ inflection at B^* might be a signature of Fermi-surface instability due to the breakdown of Kondo effect [18]. Notably, in line with the field-insensitive FL-like $\rho(T)$ at $T < 2$ K [Fig. 4(b)], the $\rho(B)$ curves for lower temperatures of $T = 0.3$ and 1 K reveal a monotonic increase with field [Fig. 5(b)] without detectable signature at B^*. These results strongly support the proposition of a pseudodoublet ground state with finite-energy spacing. As such, it turns out clear that though an antiferromagnetic order and a pertinent quantum critical point (QCP) are absent in $PrAu_2In_4$, a field-tuned strange-metal behavior emerges at low but finite temperatures of $T > 2$ K.

To further elucidate the unique low-energy thermodynamics, in Fig. 6(a) we compare the specific heat $C(T)$ between $PrAu_2In_4$ and $LaAu_2In_4$. The latter compound is well described by Debye's description $C/T = \gamma + \beta T^2$, with a small Sommerfeld coefficient $\gamma = 5.0$ mJ mol^{-1} K^{-2} and $\beta = 2.5$ mJ mol^{-1} K^{-4}. By contrast, $PrAu_2In_4$ shows two marked

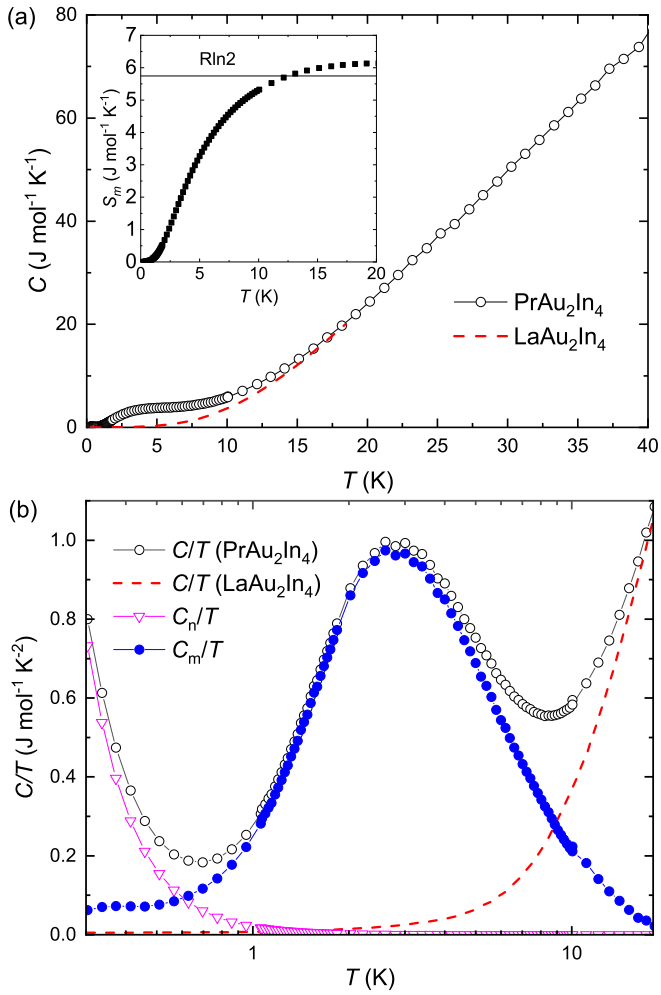

FIG. 6. (a) Specific heat $C(T)$ of $PrAu_2In_4$ and $LaAu_2In_4$. Inset: Magnetic entropy $S_m(T)$ of $PrAu_2In_4$ calculated by integrating $C_m(T)/T$. (b) The as-measured $C(T)/T$, the estimated nuclear contribution C_n/T, and the magnetic contribution C_m/T. The latter value saturates to $\gamma \approx 70$ (± 20) mJ mol^{-1} K^{-2} at $T < 0.5$ K.

features at low temperatures: A broad $C(T)$ maximum at $T \sim 3$ K and an upturn at $T < 0.7$ K, which are better revealed in the C/T vs log T plot in Fig. 6(b). The $C(T)$ maximum has a long tail extending to above 10 K and is too broad to be ascribed to a magnetic order. Given the enhanced VV susceptibility observed at low temperatures, it is reasonable to interpret this broad feature as a Schottky anomaly arising from thermal population of the $4f$ pseudodoublet ground state. The C/T upturn at $T < 0.7$ K is a high-T tail of the Schottky anomaly of Pr nuclear magnetic moment ($I = 5/2$) exposed in the hyperfine field of surrounding $4f$ electrons [19]. It therefore offers strong, although indirect, evidence of significant exchange coupling arising from the mixing between the ground and the low-lying singlets. Assuming the magnetic specific heat C_m/T takes a constant value at the lowest temperatures, the nuclear part, which follows $C_n/T = A_n T^{-3}$, can be obtained by simulating the as-measured C/T with the sum of C_m/T, C_n/T, and C_l/T. Here, the lattice contribution C_l/T is approximated by the as-measured C/T of $LaAu_2In_4$. The simulated results are shown in Fig. 6(b),

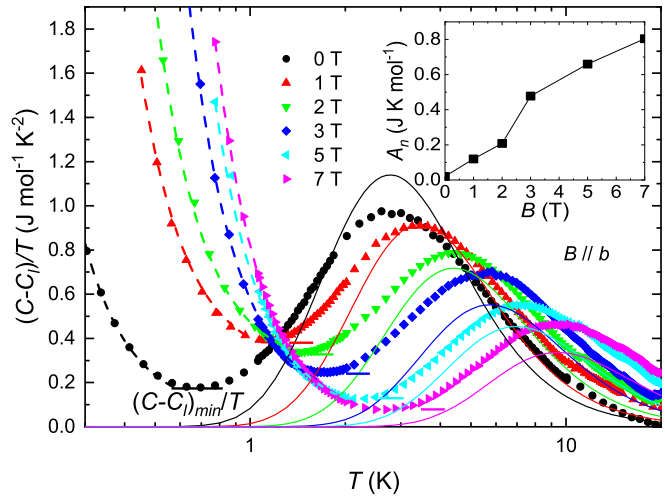

FIG. 7. $(C - C_l)/T$ vs T, i.e., the sum of magnetic and nuclear specific heat, measured in varied fields for $PrAu_2In_4$. By fitting the broad Schottky anomaly to a simple two-level model (see the solid lines), one obtains the splitting energy Δ_E between the ground and the low-lying singlet. The short horizontal bar marks the $(C - C_l)/T$ value at the minimum, defined as $(C - C_l)_{\rm min}/T$. Inset shows the value of A_n as a function of magnetic field that is obtained by fitting the low-temperature specific-heat upturns (see the dashed lines in the main panel).

where $C_n(T)$ dominates the measured specific heat at $T < 0.5$ K, and $C_m(T)/T$ displays a large maximum at $T \approx 3$ K that can be fitted to a Schottky anomaly $4f$ pseudodoublet state (to be further discussed below with its field dependence considered). At $T < 0.5$ K, $C_m(T)/T$ tends to flatten out to a constant value $\sim$70 ($\pm$20) mJ mol^{-1} K^{-2}, which is defined as the electronic specific heat coefficient γ of $PrAu_2In_4$. The moderately enhanced value of γ, relative to the small γ ($= 5.0$ mJ mol^{-1} K^{-2}) value of $LaAu_2In_4$, can be attributed to the hybridization between the conduction band and the local excitations of the pseudodoublet state. The pseudodoublet ground state is also confirmed by the magnetic entropy $S_m(T)$, obtained by integrating C_m/T with respect to T [Fig. 6(a) inset]. Here, $S_m = R \ln 2$ (R is the gas constant) associated with the full entropy of the pseudodoublet ground state is reached already at a rather low temperature of $T \sim 13$ K.

Figure 7 displays $(C - C_l)/T$ vs T measured in varied fields for $PrAu_2In_4$. Here, $(C - C_l)/T$ is the as-measured C/T minus the lattice part, comprising the sum of the magnetic and nuclear contributions. The broad Schottky anomaly observed at $T \approx 3$ K for $B = 0$ shifts to higher temperature with increasing field. Accordingly, the energy gap characterizing the pseudodoublet spacing, which is estimated to be $\Delta_E \approx 9$ K by fitting the anomaly with a two-level model, grows up quasilinearly with field as expected for Zeeman splitting. This is a common feature observed in many heavy-fermion systems when the antiferromagnetic order (if any) is suppressed by field (see, for example, CePdAl [20]), suggestive of the magnetic character of the pseudodoublet in $PrAu_2In_4$. Note that the two-level calculation overestimates the Schottky anomaly in zero field, hinting at the involvement of the Kondo physics that will broaden the Schottky anomaly (Fig. 7). The

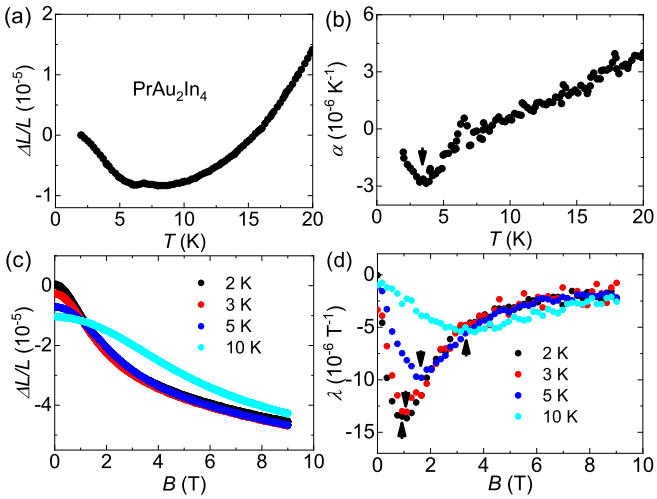

FIG. 8. (a) Relative length change $\Delta L/L$ and (b) the linear thermal expansion coefficient α versus temperature measured along b axis, i.e., the needle direction. (c) Isothermal relative length change $\Delta L/L$ versus field and (d) the corresponding linear magnetostriction coefficient λ. Arrows mark the positions of $\lambda(B)$ minima, defined as B^*.

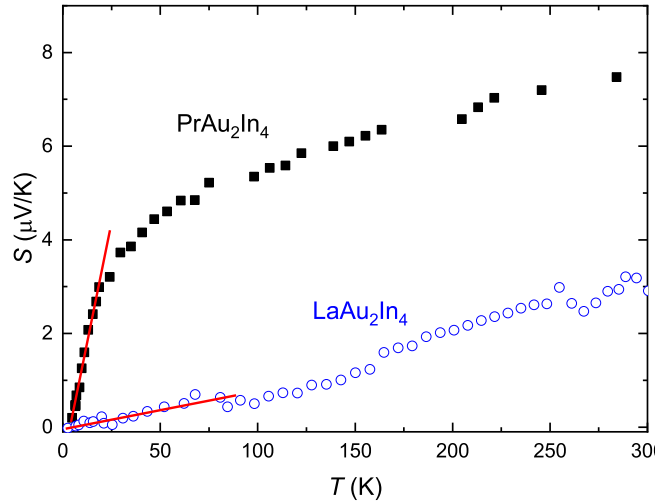

FIG. 9. The thermopower $S(T)$ of $PrAu_2In_4$ and $LaAu_2In_4$ measured along b axis. Note their very different initial slopes marked by red lines.

calculated curve for higher fields becomes gradually smaller than the as-measured one due to, on one hand, the weakened Kondo effect in field, and on the other, the increasing contribution of higher CEF levels.

The low-T $(C - C_l)/T$ upturn in all fields is further fitted to the sum of C_n/T and C_m/T as mentioned above to obtain the field dependence of A_n and γ. The fitting results are shown as dashed lines in Fig. 7. As shown in Fig. 7 inset, A_n increases monotonically with field, whereas $\gamma(B)$ reveals a broad maximum at 1–2 T [to be shown in Fig. 10(b)]. Actually, the nonmonotonic change of $\gamma(B)$ can also be straightforwardly inferred from the evolution of $(C - C_l)/T$ minimum, $(C - C_l)_{\min}/T$, without resorting to any numerical fitting. The value of $(C - C_l)_{\min}/T$, marked by the horizontal bar in Fig. 7, shifts gradually to higher temperature and lower value with increasing field from $B = 1$ T to 7 T, whereas for $B = 0$, $(C - C_l)_{\min}/T$ occurs at the lowest temperature with the lowest value among all measurements, in line with the fitted $\gamma(B)$ result.

The inference drawn above is further supported by thermal expansion and magnetostriction measurements. The relative length change $\Delta L/L$ measured along b for $PrAu_2In_4$ reveals a broad minimum around 8 K, and correspondingly, the linear thermal expansion coefficient, defined as $\alpha = \mathrm{d}(\Delta L/L)/\mathrm{d}T$, changes sign in this vicinity [see Figs. 8(a) and 8(b)]. A minimum is observed in $\alpha(T)$ at 3 K, matching T_{cro} determined from $\mathrm{d}(M/B)/\mathrm{d}T$. This indicates that the negative $\alpha(T)$ at low temperatures is dominated by thermal depopulation of the pseudodoublet state, rather than the competition between Kondo effect and RKKY interaction as observed in typical heavy-fermion compounds [21]. By measuring the field dependence of $\Delta L/L$, i.e., the magnetostriction, one can easily identify the crossover field B^* by locating the minimum in magnetostriction coefficient $\lambda(B) = \mathrm{d}(\Delta L/L)/\mathrm{d}B$ [Figs. 8(c) and 8(d)]. That is, the slope of $\Delta L/L$ experiences a drastic change at B^*, whose values show excellent agreement with those determined from the $\rho(B)$ curves (Fig. 5). In fact, the crossover field that marks the Fermi-surface instability in $YbRh_2Si_2$ was also determined by the similar features of $\lambda(B)$ and $\rho(B)$ [17].

Figure 9 compares the thermopower $S(T)$ of $PrAu_2In_4$ and $LaAu_2In_4$. A remarkable difference is seen in their initial slopes S/T at low temperatures, as marked by red lines. The slope for $PrAu_2In_4$, 0.177 $\mu V/K^2$, is larger than that of $LaAu_2In_4$, 0.008 $\mu V/K^2$, by a factor of $\sim$20. Recalling the γ values of the two compounds differing by a similar ratio, we interpret the thermopower of $PrAu_2In_4$ as important transport evidence of Kondo hybridization in this compound [22].

Figure 10(a) displays the contour map of the resistivity curvature characterized by $\mathrm{d}^2\rho/\mathrm{d}T^2$ in a T-B phase space to illustrate the field-induced strange metal behaviors. T_{cro}, which denotes the crossover temperature in $M(T)/B$, and $\Delta_E/2k_B$ that measures the activation energy of the Zeeman-split pseudodoublet, as well as B^* detected by the isothermal resistivity and magnetostriction, are shown to construct a quantum critical "phase diagram." Among them, T_{cro} and $\Delta_E/2k_B$ characterize the energy spacing of the pseudodoublet. They show finite values already at $B = 0$ and increase almost linearly with field. In contrast, B^* is inferred to be the crossover field where Fermi-surface instability might take place [2]. Its temperature dependence hints at a hypothetical QCP at $B_{cri} < 1$ T when $T \to 0$ if the ground state were a true doublet, supported by the contour map where a negative-to-positive $\rho(T)$ curvature change is observed at low fields. In Fig. 10, we leave the $T < 2$ K regime blank, where the thermal population of the low-lying singlet is negligible and FL-like behavior persists across the field window studied.

In Fig. 10(b), we corroborate the finite-T strange-metal behavior by presenting $\gamma(B)$ estimated by fitting the low-T $(C - C_l)/T$ upturn, which shows a broad maximum near 1–2 T. In support of this estimation, we also show $(C - C_l)_{\min}/T$ directly read from the minimum of $(C - C_l)/T$ vs T (short

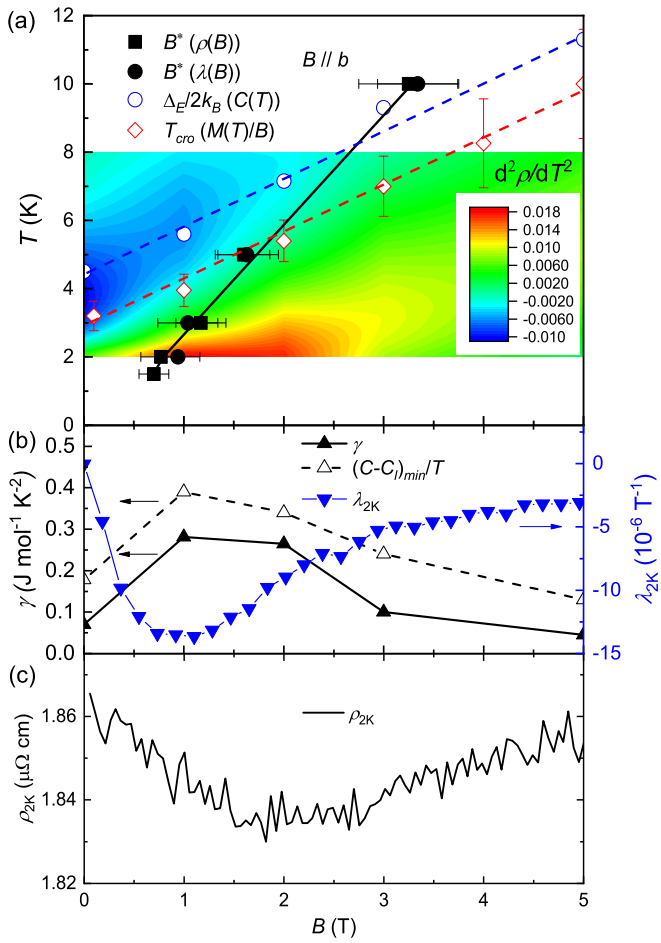

FIG. 10. (a) T-B "phase diagram" of $PrAu_2In_4$ on top of the contour map of the $\rho(T)$ curvature characterized by $d^2\rho/dT^2$. T_{cro}, detected by the $M(T)/B$ shoulder, and $\Delta_E/2k_B$, which measures the activation energy of the Zeeman-split pseudodoublet, are shown to illustrate the evolution of the energy spacing of the pseudodoublet in field. The crossover field B^* determined from the isothermal $\rho(B)$ and $\lambda(B)$ are also shown. (b) The values of the ground-state Sommerfeld coefficient γ, $(C - C_l)_{\rm min}/T$ (see Fig. 7 for its definition), as well as the isothermal magnetostriction coefficient $\lambda(B)$ and (c) $\rho(B)$ measured at 2 K are plotted as a function of field.

horizontal bar in Fig. 7), as a convenient measure to track the evolution of the ground-state Sommerfeld coefficient. Similarly, the low-T magnetostriction coefficient $\lambda_{2K}(B)$ shows a broad minimum at ∼1 T, akin to the isothermal resistivity $\rho_{2K}(B)$ shown in Fig. 10(c). These transport and thermodynamic signatures collectively support the presence of strange metal across an extended field range near and below 2 T, pointing to a probable Fermi-surface instability in $PrAu_2In_4$ originating from the competition between Kondo physics and exchange interaction. Otherwise, it would be difficult to explain the field-induced crossover features solely by the increasing energy spacing $\Delta_E(B)$ of the pseudodoublet.

While absent in $PrAu_2In_4$, magnetic order arising from the mixing of ground and low-lying singlets has been reported for a large number of Pr-based compounds of orthorhombic symmetry. These include, for example, PrPtAl [23], which has a ferromagnetic order at $T_C = 5.8$ K and the singlet-singlet CEF splitting $\Delta_E = 21$ K, $PrFe_2Al_8$ [24] with an antiferromagnetic order at $T_N \approx 4$ K and $\Delta_E \approx 10$ K, $PrAgAl_3$ [25] ($T_C = 5.8$ K, $\Delta_E = 15$ K), Pr_3Al_{11} [26] ($T_{N1} = 12.6$ K, $T_{N2} = 3.1$ K, and $\Delta_E = 4.2$ K), $PrCo_2Ga_8$ [27] with an antiferromagneticlike transition at 1.28 K, and so on. In all these systems, the magnetic exchange energy is comparable to or slightly higher than the lowest CEF splitting energy, resulting in a significant admixture of the ground and the first CEF singlet, giving rise to cooperative magnetism. Exploring how the quantum critical regime manifests itself when the thermally induced magnetic order observed in these systems is suppressed to zero remains an interesting topic for future investigation.

IV. SUMMARY AND CONCLUSION

Summarizing the experiments, $PrAu_2In_4$ has a pseudodoublet ground state in the orthorhombic CEF, with strong magnetocrystalline anisotropy leading to an Ising-like spin degree of freedom along b axis, i.e., the needle direction. Our detailed studies indicate this compound lies in close proximity to cooperative magnetism arising from the exchange interaction of $4f$ electrons, which competes with not only the Kondo effect, but also the CEF energy between the closely spaced ground and the lowest-lying singlets.

Moreover, in the temperature range of about 2 K $< T <$ 10 K, the resistivity $\rho(T)$ of $PrAu_2In_4$ exhibits a high field tunability, displaying a curvature change and a quasilinear variation across a wide range of external field near 1–2 T. Such a strange-metal $\rho(T)$ behavior gradually changes into FL-like at $B > 2$ T, where T-quadratic resistivity is restored. While observed only at finite temperatures, these features bear strong resemblance to the quantum critical behaviors frequently observed near a magnetic QCP in heavy-fermion compounds. However, cooling $PrAu_2In_4$ to below 2 K reveals that its ground state becomes insensitive to field and exhibits FL-like behavior in all fields due to the thermal depopulation of the low-lying singlet. Consistent with these results, signature of finite-T quantum crossover is obtained in the isothermal $\rho(B)$ measured at $T \geqslant 1.5$ K, which markedly drops at a crossover field B^*, resembling the quantum critical signature observed in $YbRh_2Si_2$. Furthermore, both the electronic specific-heat coefficient γ and the magnetostriction coefficient λ also display a broad maximum/minimum at $B \sim$ 1–2 T. Taken together, these experimental observations suggest that the metallic Fermi surface in $PrAu_2In_4$ might experience a fluctuation near the crossover field B^* at finite temperatures, whereas the ground state appears to consistently be Fermi liquid.

The estimated low-temperature Sommerfeld coefficient $\gamma \approx 70\,(\pm 20)$ mJ mol^{-1} K^{-2} indicates a moderate mass enhancement in $PrAu_2In_4$ due to the Kondo effect acting on the ground-state pseudodoublet of Pr^{3+}, which is further evidenced by the enhanced initial thermopower slope S/T relative to that of $LaAu_2In_4$. In addition, the Kadowaki-Woods ratio A/γ^2 is estimated to be 2.5×10^{-6} μΩ cm (K mol/mJ)^2, close to that of its Ce-based counterpart $CeAu_2In_4$ [8]. Given the accumulated signatures of finite-temperature quantum fluctuations arising from the competing multiple energy scales including the pseudodoublet spacing, the Kondo effect, and

the RKKY exchange interaction, the quantum critical "phase diagram" of $PrAu_2In_4$ offers a fertile ground for studying heavy-fermion and emergent quantum criticality related to accidental and quasidegenerate ground-state multiplet of non-Kramers ions.

ACKNOWLEDGMENTS

The authors are grateful to Y.-F. Yang and W. Li for discussions. This work was supported by the National Natural Science Foundation of China (Grants No. 12141002 and No. 52088101), the National Key R&D Program of China (Grants No. 2022YFA1402200, No. 2021YFA0718700, No. 2023YFA1406000, and No. 2022YFA1602802), and the Chinese Academy of Sciences through the Project for Young Scientists in Basic Research (Grant No. YSBR-057), the Strategic Priority Research Program (Grant No. XDB33000000), and the Scientific Instrument Developing Project (Grant No. ZDKYYQ20210003). A portion of this work was carried out at the Synergetic Extreme Condition User Facility (SECUF) in Beijing.

[1] G. R. Stewart, Heavy-fermion systems, Rev. Mod. Phys. **56**, 755 (1984).
[2] Q. Si and F. Steglich, Heavy fermions and quantum phase transitions, Science **329**, 1161 (2010).
[3] J. A. Mydosh and P. M. Oppeneer, *Colloquium:* Hidden order, superconductivity and magnetism: The unsolved case of URu_2Si_2, Rev. Mod. Phys. **83**, 1301 (2011).
[4] E. D. Bauer, N. A. Frederick, P.-C. Ho, V. S. Zapf, and M. B. Maple, Superconductivity and heavy fermion behavior in $PrOs_4Sb_{12}$, Phys. Rev. B **65**, 100506(R) (2002).
[5] T. Onimaru and H. Kusunose, Exotic quadrupolar phenomena in non-Kramers doublet systems – the cases of PrT_2Zn_{20} (T = Ir, Rh) and PrT_2Al_{20} (T = V, Ti) –, J. Phys. Soc. Jpn. **85**, 082002 (2016).
[6] J. R. Salvador, K. Hoang, S. D. Mahanti, and M. G. Kanatzidis, $REAu_2In_4$ (RE = La, Ce, Pr, Nd): Polyindides from liquid indium, Inorg. Chem. **46**, 6933 (2007).
[7] D. A. Joshi, P. Manfrinetti, S. K. Dhar, and A. Thamizhavel, Magnetic anisotropy in single crystalline $CeAu_2In_4$, J. Phys.: Conf. Ser. **200**, 012074 (2010).
[8] M. Lyu, H. Zhao, J. Zhang, Z. Wang, S. Zhang, and P. Sun, $CeAu_2In_4$: A candidate of quasi-one-dimensional antiferromagnetic Kondo lattice, Chin. Phys. B **30**, 087101 (2021).
[9] S. Sarkar, M. J. Gutmann, and S. C. Peter, Crystal structure and magnetic properties of indium flux grown $EuAu_2In_4$ and $EuAuIn_4$, Cryst. Growth Des. **13**, 4285 (2013).
[10] S. Akamaru, Y. Isikawa, J. Sakurai, K. Maezawa, and H. Harima, Magnetic properties and de Haas– van Alphen effect of $PrNi_2Al_5$, J. Phys. Soc. Jpn. **70**, 2049 (2001).
[11] G. T. Trammell, Magnetic ordering properties of rare-earth ions in strong cubic crystal fields, Phys. Rev. **131**, 932 (1963).
[12] T. Naka, L. A. Ponomarenko, A. de Visser, A. Matsushita, R. Settai, and Y. Ōnuki, Ordered magnetic and quadrupolar states under hydrostatic pressure in orthorhombic $PrCu_2$, Phys. Rev. B **71**, 024408 (2005).
[13] Y. Kusanose, T. Onimaru, G.-B. Park, Y. Yamane, K. Umeo, T. Takabatake, N. Kawata, and T. Mizuta, Hindered quadrupole order in $PrMgNi_4$ with a nonmagnetic doublet ground state, J. Phys. Soc. Jpn. **88**, 083703 (2019).
[14] T. Morie, T. Sakakibara, H. S. Suzuki, H. Tanida, and S. Takagi, Unusual low-temperature magnetization of a cubic Γ_3 non-Kramers doublet ground state compound $PrMg_3$-evidence of a hybridization effect, J. Phys. Soc. Jpn. **78**, 033705 (2009).
[15] T. Sakakibara, T. Morie, H. S. Suzuki, T. Tanida, S. Takagi, and T. Onimaru, Low-temperature magnetization of $PrMg_3$ with a Γ_3 non-Kramers doublet ground state, J. Phys.: Conf. Ser. **200**, 012171 (2010).
[16] H. Ishii, Nuclear magnetism in Van Vleck metals, J. Low Temp. Phys. **135**, 579 (2004).
[17] P. Gegenwart, T. Westerkamp, C. Krellner, Y. Tokiwa, S. Paschen, C. Geibel, F. Steglich, E. Abrahams, and Q. Si, Multiple energy scales at a quantum critical point, Science **315**, 969 (2007).
[18] Q. Si, S. Rabello, K. Ingersent, and J. L. Smith, Locally critical quantum phase transitions in strongly correlated metals, Nature (London) **413**, 804 (2001).
[19] A. K. Pathak, D. Paudyal, Y. Mudryk, K. A. Gschneidner, Jr., and V. K. Pecharsky, Anomalous Schottky specific heat and structural distortion in ferromagnetic $PrAl_2$, Phys. Rev. Lett. **110**, 186405 (2013).
[20] S. Lucas, K. Grube, C.-L. Huang, A. Sakai, S. Wunderlich, E. L. Green, J. Wosnitza, V. Fritsch, P. Gegenwart, O. Stockert, and H. V. Löhneysen, Entropy evolution in the magnetic phases of partially frustrated CePdAl, Phys. Rev. Lett. **118**, 107204 (2017).
[21] Z. Zhuang, M. Lyu, T. Zhang, X. Zhang, Z. Wang, H. Zhao, J. Xiang, Y. Isikawa, S. Zhang, and P. Sun, Magnetism in frustrated Kondo and non-Kondo intermetallics: $CeInCu_2$ versus $NdInCu_2$, Phys. Rev. B **107**, 195154 (2023).
[22] K. Behnia, D. Jaccard, and J. Flouquet, On the thermoelectricity of correlated electrons in the zero-temperature limit, J. Phys.: Condens. Matter **16**, 5187 (2004).
[23] H. Kitazawa, H. Suzuki, H. Abe, J. Tang, G. Kido, and A. Dönni, Magnetic properties of induced ferromagnet PrPtAl, J. Appl. Phys. **85**, 4480 (1999).
[24] H. S. Nair, S. K. Ghosh, K. R. Kumar, and A. M. Strydom, Magnetic ordering and crystal field effects in quasi-caged structure compound $PrFe_2Al_8$, J. Phys. Chem. Solids **91**, 69 (2016).
[25] S. Nallamuthu, A. Dzubinska, M. Reifffers, and J. R. Fernandez, Ferromagnetism in orthorhombic $RAgAl_3$ (R = Ce and Pr) compounds, Phys. B: Condens. Matter **521**, 128 (2017).
[26] C. S. Garde, T. Takeuchi, Y. Nakano, Y. Takeda, Y. Ota, Y. Miyauchi, K. Sugiyama, M. Hagiwara, K. Kindo, F. Honda, R. Settai, and Y. Ōnuki, Electrical and magnetic properties of R_3Al_{11} (R = La, Ce, Pr, and Nd), J. Phys. Soc. Jpn. **77**, 124704 (2008).
[27] M. O. Ogunbunmi, B. M. Sondezi, H. S. Nair, and A. M. Strydom, Electronic and magnetic properties of quasi-skutterudite $PrCo_2Ga_8$ compound, Phys. B: Condens. Matter **536**, 128 (2018).